Tool for simulating tumor growth in various regions of the human body in three dimensions.

Carlos Carret Miranda
University of Havana
carlos.carret@estudiantes.matcom.uh.cu

Reinaldo Rodríguez Ramos
Department of Mathematics, Faculty of Mathematics and Computer Science, University of Havana, Cuba, and PPG-MCCT, Federal Fluminense University, Volta Redonda, Rio de Janeiro, Brazil.
reinaldo@matcom.uh.cu and reinaldorr@id.uff.br

Panters Rodríguez Bermúdez
Departamento de Ciências Exatas, Universidade Federal Fluminense, Volta Redonda, Rio de Janeiro, Brazil
pantersrb@id.uff.br

Summary: Cancer is a disease characterized by the uncontrolled growth of abnormal cells in the body. It is a complex and multifaceted disease that has challenged researchers and doctors for decades. The ability to visualize and understand tumor growth can provide valuable insights into how cancer develops and spreads, leading to significant improvements in cancer diagnosis, treatment, and prevention. The three-dimensional tumor growth simulation tool that is being developed is an important step in this direction. It allows for detailed visualization of tumor growth in different parts of the human body, which can provide valuable insights into how cancer develops and spreads. Additionally, the ability of this tool to simulate tumor growth in different parts of the body means that it can be used to study a wide range of cancer types. This tool utilizes a cellular automaton and a small-world network to create connections between cells, allowing for a more accurate representation of organ and tumor structures. Furthermore, it allows for the loading of configurations and parameters from external files, providing great flexibility to the tool and allowing for customization of the simulation to the specific needs of each case. For 3D rendering, the Marching Cubes technique is used, which enables detailed and accurate three-dimensional representation of tumors.

Keywords: Scientific Computing, Numerical Methods, and Applications. Cellular Automaton. Marching Cubes. 3D. Cancer.

Introduction

The challenge of representing biological phenomena mathematically, physically, and computationally requires interdisciplinary synergy among experts in these fields. This collaboration enriches the traditional experimental method used in biological sciences by implementing mathematical models, which serve as tools to formulate and test hypotheses, guide experimental research, and refine the model based on the obtained results (1).

Cancer is a disease that affects a large number of living organisms and is characterized by the presence of a group of abnormal cells that grow uncontrollably, disregarding the normal rules of cell division. It particularly affects humans, where its occurrence and development pose a threat to life. The malignancy of cancer varies and depends on factors such as the growth rate of cancer cells, their ability to spread to other tissues, and the possibility of recurrence after surgical removal (1).

The purpose of this type of research is to achieve a deeper understanding of biological processes through an iterative cycle of theory and experimentation. Additionally, mathematical models can be used to assist in the conception and design of therapeutic strategies, providing a more precise and personalized insight into the treatment of each patient (1).

In the case of this project, a cellular automaton and a small-world network are used to model the interactions between cells, providing a more accurate representation of tumor growth. The parameters and configurations can be loaded from external files, offering great flexibility in adapting the simulation to the specific needs of each case. The work being conducted is a part of a bachelor thesis project recently presented and concluded. The project aims to simulate tumor growth in small organs and involves loading and utilizing parameters for the simulation. The graph of cells with their connections is visualized and analyzed, along with the visualization of the tumor size throughout the simulation. The focus of the next stages is to improve the existing implementation and incorporate changes based on details found in medical literature. Additionally, efficient algorithms will be implemented to process large amounts of cells and their connections. In the future, the project aims to incorporate Artificial Intelligence and Machine Learning techniques to achieve better approximations to reality.

The technique of Marching Cubes (2) is used for 3D rendering, providing a detailed and precise visualization of tumors. This visualization can provide valuable insight into how cancer develops and spreads, which can be essential for the development of effective therapies and treatments. By visualizing tumor growth in three dimensions, doctors and scientists can gain a better understanding of tumor evolution and how it may affect surrounding tissues. This information can be crucial for the development of effective therapies and treatments for cancer.5

Definition of the model

Cellular Automaton

In this section, the cellular automaton model presented in this work is conceived. It begins by formally defining a cellular automaton (1).

A cellular automaton is a tuple $(\mathscr{L};\mathscr{N};\mathscr{E};\mathscr{R})$ composed of the following representative elements (3):

$\mathscr{L}$: It is a potentially infinite set of cells.

$\mathscr{N}$: $\mathscr{L}\times\mathscr{L}\to\{0,1\}$ is a neighborhood function, which can be seen as a relation, usually reflexive and symmetric, between cells. This function shows which pairs of cells are neighbors, that is, the geometry of the cellular organization.

$\mathscr{E}$: It is a set of states. Each cell in the set $\mathscr{L}$ is assigned an associated state at each time step.

$\mathscr{R}$: $\mathscr{E}^{|\mathscr{N}(v)|}\to\mathscr{E}$ is a locally defined transition function. This function is the core of the dynamics of a cellular automaton and is commonly expressed through rules that define the state of the cell in the next time step based on the state of the neighboring cells. The set containing the state of the neighboring cells is obtained through the function $\mathscr{N}(v)$, which is defined below.

En el presente trabajo se utiliza la notación empleada en (3) In this work, the notation used in (3) is employed

Model Hypothesis

Cancer is an extremely complex disease composed of a large number of processes, cellular interactions, and factors. As part of the modeling process, it is necessary to achieve a simplification of the problem to make it tractable, based on reducing reality to a set of hypotheses.

To test the efficiency of our tool, we will use a cellular automaton model, which is based on certain general hypotheses that will be presented next. This model focuses on the type of cancer known as carcinoma or epithelial cell carcinoma.

I. **Idealized progression of tumor development**: *It is assumed that tumor development follows an idealized progression divided into the avascular and vascular stages, where the macroscopic behavior of the tumor is defined by the mutations expressed by cancerous cells.*

II. **Mutations of cancer cells**: *It is assumed that the accumulation of mutations in the cancer cell is defined as a sequential process and follows an established order, i.e., during the avascular stage, mutations related to the cell cycle and tumor growth are expressed, and during the vascular stage, mutations related to angiogenesis and metastasis are expressed, in addition to the previous ones.*

III. **Biological entities of the model**: *The biological entities present in the model consist only of the types of cells defined in the set of states of the cellular automaton, which consists of three cell populations: normal cells, cancerous cells, and immune cells.*

IV. **Interactions between model entities**: *The interactions between the different cells of the model consist solely of the rules defined in the transition function of the automaton. There are types of cell actions that are considered regarding cell movement: cell proliferation and two types of interactions in the system of the model, between the normal cells and the cancerous cells, and between the cancerous cells and immune cells.*

V. **Invariance of normal cells**: *It is assumed that the population of normal cells in the body is static and invariant over time, that is, they do not undergo cell division or death processes.*

VI. **Homogeneity of cancer cells**: *It is assumed that the population of cancer cells that forms a tumor mass is homogeneous, that is, there are no subtypes with different mutations or that are at different stages of the cell cycle.*

VII. **Sufficiency of nutrients**: *It is assumed that the supply of nutrients and oxygen is constant and sufficient so that all the tumors represented in the cellular automaton develop properly.*

VIII. **Tumor development in relation to the population**: *It is assumed that the advancement of a tumor through its different development stages depends uniquely on its cell population, described by Verhulst's logistic growth equation.*

IX. **Simple growth process**: *Tumor development is represented by a simple growth process, that is, a position occupied by one of these cancerous cells remains occupied in the remaining time instances, except that the cancerous mass to which they belong is removed from the simulation as occurs with metastases.*

X. **Cell adhesion**: *It is assumed that the adhesion of cancerous cells is maintained at all times except for detachments of migratory cells as part of the metastatic cascade.*

XI. **Metastasis paths**: *Only hematic and lymphatic dispersion is considered as the pathways of metastasis.*

XII. **Tissue representation**: *It is assumed that a tissue can be represented by a small world network, generated from the Watts-Strogatz model where the coordinates of the vertices have two components $x, y \in \mathbb{N}$ that constitute the location of the cell in the corresponding plane with a cut of said tissue.*

XIII. **Support or stroma tissues**: *All the support tissues of an organ are simply represented as stroma because only two fundamental interactions between healthy tissues and cancer are considered: invasion and migration. Therefore, it is not necessary to distinguish between the different layers of support.*

XIV. Neovascularization interpretation: *It is assumed that the neovascularization that grows inside a tumor due to angiogenesis produces an increase in the capacity load of the environment and in the rate of proliferation of the tumor itself.*

XV. Competitive tumor situations: *In situations of competition among several tumors to expand into the same position, it is assumed that the value of the transition probability corresponds to the tumor with the highest likelihood of expansion at that moment. If the tumor eventually expands towards that position successfully, the new cancerous cell belongs to that tumor.*

XVI. Nutrient concentration vectors: *It is assumed that the concentration of nutrients increases as we approach the support tissues and the organism's vasculature. This fact is represented by one or more vectors in the organs of the set of cells of the automaton that indicates the directions in which the nutrient concentration increases.*

XVII. Directional bias of tumor growth: *It is assumed that the probability of increasing the cell population of a tumor is affected by the concentration of nutrients. This fact constitutes a bias in the direction of tumor growth, which translates into a tendency to expand towards higher concentration.*

XVIII. **Tumor expansion speed:** *It is assumed that the speed of tumor expansion depends on the distance between the cancer cells and the healthy cell trying to displace it, which decreases as the distance increases.*

XIX. Cancer migration: *In this model, only the migration of individual cells is represented and no distinction is made between their different modes. In addition, it is considered that during their displacement these cells do not divide.*

XX. Directional bias of migration: *The displacement of migrant cells across the ECM of the stroma is conditioned by the nutrient concentration vectors, which are determinants in the selection of the direction of their movement. The process of ECM degradation is not represented in this model.*

XXI. **Distant connections of the graph**: *Each represented organ is linked to the others through the distant connections existing in the underlying graph. It is assumed that a cell that penetrates the circulatory system at a given point will leave it in a predetermined position, corresponding to the destinies of the mentioned connections.*

XXII. **Viable destinations of metastasis**: *Only the migrations of cancerous cells towards locations that are uncolonized or correspond to a micrometastasis are represented. If the target locations correspond to a tumor, the migrating cell leaves its position and enters the circulatory system but its transport and arrival at the new location are not evaluated.*

XXIII. Competitive situations between micrometastases: *In situations of competition among various micrometastases to expand into the same position, it is assumed that the value of the transition probability corresponds to the micrometastasis with the highest likelihood of expansion at that moment.*

XXIV. **Immune cells**: *Each represented organ is linked to the others through the distant connections existing in the underlying graph. It is assumed that a cell that penetrates the circulatory system at a given point will leave it in a predetermined position, corresponding to the destinies of the mentioned connections.*

Neighborhood function

The sets $A^n(G)$ and $A^d(G)$ group the edges of the graph that correspond to immediate and distant connections, respectively. These sets have the following properties:

$$A^n(G) \cup A^d(G) = A(G), \tag{1a}$$

$$A^n(G) \cap A^d(G) = \emptyset. \tag{1b}$$

These properties indicate that the subsets of edges $A^n(G)$ and $A^d(G)$ form a partition of the set of edges $A(G)$

Based on the sets of vertices $V(G)$ and edges $A(G)$, the representative elements $\mathscr{L}$ and $\mathscr{N}$ of the cellular automaton model are defined as follows:

The set of cells $\mathscr{L}$ is defined based on the set of vertices of the graph $V(G)$:

$$\boxed{\mathscr{L} = V(G)}. \tag{2}$$

The neighborhood function $\mathscr{N}$ s defined based on the set of edges of the graph $A(G)$ as shown below:

$$\boxed{\mathscr{N} : V(G) \times V(G) \to \{0,1\}}, \tag{3a}$$

$$\boxed{\mathscr{N}(v,w) = \begin{cases} 0 & if\ \{v,w\} \notin A(G) \\ 1 & if\ \{v,w\} \in A(G) \end{cases}}, \tag{3b}$$

In other words, the vertices $v \in V(G)$ and $w \in V(G)$ are neighbors in the cellular automaton if there exists an edge in G that connects them.

The neighborhood of the vertex $v \in V(G)$ is defined based on the neighborhood function $\mathscr{N}(v,w)$ as the set of vertices $\mathscr{N}(v)$ that have edges with the vertex v:

$$\mathscr{N}(v) = \{w \mid \mathscr{N}(v,w) = 1\}. \tag{4}$$

*Set of cells: Watts-Strogatz model

In the presented study, a soft tissue is defined as a set of cells that exhibit two types of connections: between nearby neighboring cells and between distant cells. To represent these types of connections, a cellular automaton model based on a graph network is used. In their work (4), Duncan J. Watts and Steven H. Strogatz showed that there are many biological, technological, and social networks that lie between regular and random networks, which have traditionally been used to model different types of dynamic systems.

Let v be a vertex of the graph that has k_v edges connecting it to k_v vertices. The value between the actual number of edges K_v that exist between these k_v vertices and the maximum number of possible edges[1] $k_v(k_v-1)/2$ is the clustering coefficient of vertex v and is determined as (1):

$$C_v = \frac{2K_v}{k_v(k_v-1)}. \tag{5}$$

The global clustering coefficient of the graph C_G is the average of all individual clustering coefficients C_v, that is (1):

$$C_G = \frac{1}{|V(G)|} \sum_{v=1}^{|V(G)|} C_v. \tag{6}$$

[1]The maximum number of possible edges is reached when the neighbors, denoted as k_v of vertex v belong to a clique. In an undirected graph, a clique is a set of vertices such that every pair of vertices is connected by an edge.

The average path length is the mean of the distances between every pair of vertices belonging to the graph and is denoted as ℓ_G. Due to the existence of numerous distant connections through the circulatory system, the average path length in the network of cells is relatively small.

Therefore, it is hypothesized that a living tissue possesses a high clustering coefficient and a small average path length. These characteristics are characteristic of small-world networks, and they are used to represent living tissue. To generate small-world networks with these characteristics, the Watts and Strogatz model is used (4). This model starts with a graph with q vertices, each connected to k immediate neighbors, and then randomly rewires each edge of the graph with a probability p, introducing edges that connect distant vertices.

Marching Cubes

The Marching Cubes technique is a computer graphics algorithm used to extract a polygonal mesh of an isosurface from a three-dimensional discrete scalar field, such computed tomography (CT) scans and magnetic resonance imaging (MRI) data (2). In the context of this project, it is used for the three-dimensional representation of tumors, providing detailed and accurate visualization.5

This algorithm works by processing the cells of volume data (also known as voxels), checking the intersection between their respective edges and the isosurface. The values of each vertex of the cells are compared with a given isosurface value, and these vertices are classified as ”inside” or ”outside” the isosurface. Once the type of intersection is determined, an approximation of the isosurface contained in the cell is constructed by building triangles (5).

The resulting visualization can provide valuable insights into how cancer develops and spreads. By visualizing tumor growth in three dimensions, doctors and scientists can gain a better understanding of tumor evolution and how it may impact surrounding tissues. This information can be essential for the development of effective cancer therapies and treatments.

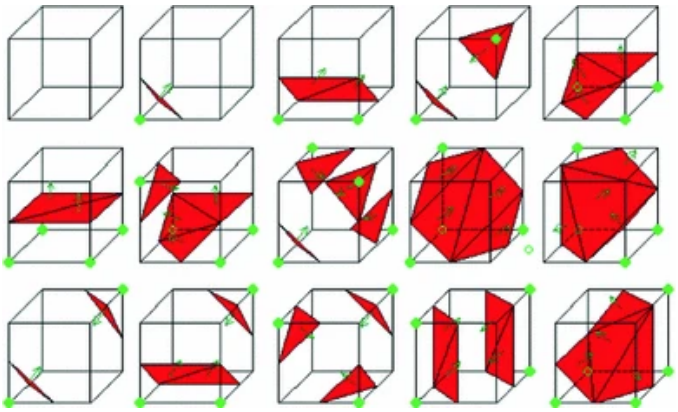

Figure 1: Illustration of the 15 basic cases of the Marching Cubes method. The green vertices are those that are classified as “inside” of the isosurfaces, while the rest is classified as “outside” of them.

Due to the high computational cost of representing and applying the Marching Cubes algorithm to realistic models containing millions of cells, this work implements a model scaling technique that reduces the length of the dimensions of the original cellular automaton model. The reduction process is as follows:

- Cells are grouped into quadrants of dimensions provided by the user.
- The states of all cells belonging to the quadrant are examined.
- The quadrant adopts the state that is most repeated among the cells in it.

- After performing this process for several quadrants, each quadrant reduces its size from $(nxmxl)$ to $(1x1x1)$, where $n \leq S_x, m \leq S_y, l \leq S_z$.

In (1) the scaling process for 2 dimensions and its influence on tumor expansion velocity are expanded upon, causing a modification in the number of days that an iteration represents. For better understanding, a visual representation is included here.(Fig.2) .

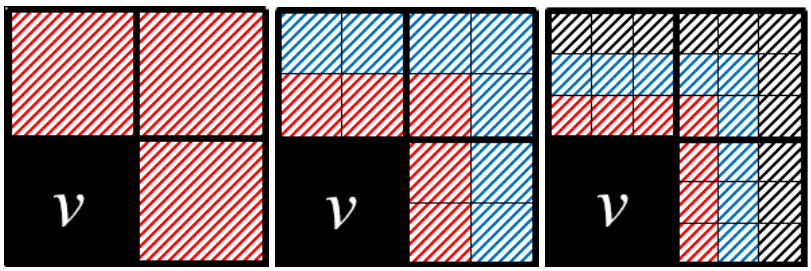

(a) Scale 1 : 1 (b) Scale 1 : 2 (c) Scale 1 : 3

Figure 2: Representation of different scales of the cellular automaton and the time spans needed for a tumor to expand satisfactorily through the space shown. Cell *v*represents a cancer cell that tries to expand to the remaining cells. The shaded areas show the minimum time needed for the tumor to occupy these cells according to the scale used. Red corresponds to 24 hours, blue to 48 hours, and black to 72 horas.hours. (a) The dimensions of a cell of the automaton are equivalent to those of a cancerous cell $3.5 \times 10^{-2} mm$. (b) The dimensions of a cell of the automaton are twice those of a cancerous cell $7.0 \times 10^{-2} mm$so each cell contains 4 células. (c) cells. (c) The dimensions of a cell of the automaton are three times those of a cancerous cell $1.05 \times 10^{-1} mm$ so each cell contains 9 cells. Images extracted from (1)

In summary, the Marching Cubes technique is a powerful tool for the three-dimensional visualization of medical data. In the context of cancer research, it can provide a detailed and accurate representation of tumor growth, which can significantly contribute to our understanding of this disease and the development of effective therapies and treatments.

State Set

Next, taking into account hypothesis XIII about support tissues, the states for the normal cells of the automaton are arranged as follows:

- $s(v,n) = 0$: The vertex v has the state corresponding to empty space or lumen at time n, and represents the hollow cavities of the organs and ducts.
- $s(v,n) = 1$: The vertex v represents an epithelial cell at time n, and corresponds to the tissue where the carcinoma originates.
- $s(v,n) = 2$:The vertex v has the state corresponding to stroma at time n, and represents the set of support tissues of the organ.

Regarding the cancerous cells, three fundamental states are distinguished based on the model hypotheses and what is explained in the section **??**:

- $s(v,n) = 3$: The vertex v represents a tumor cell at time n, and constitute the neoplastic mass.

- $s(v,n) = 4$: The vertex v represents a migrating cell at time n, that is, they have the necessary mutations to perform the metastatic cascade.
- $s(v,n) = 5$: The vertex v represents a micrometastatic cell at time n, that is, they performed the metastatic cascade successfully and are colonizing the new location, but can be destroyed by the immune system or fail in this colonization.

Finally, the states of the immune cells:

- $s(v,n) = 6$: The vertex v represents an immune cell at time n.
- $s(v,n) = 7$: The vertex v represents a cell in an intermediate state at time n.

Then the state set has the form:

$$\boxed{\mathscr{E} = \{0,1,2,3,4,5,6,7\}}\,. \tag{7}$$

Initially, each cell is assigned the corresponding state based on its position in the tissue of each location represented in the automaton, starting from the corresponding assignment of the different states. To a few primary organ epithelial cells, the corresponding state of cancerous tumor cells forming the initial neoplastic focus is assigned. The transitions between the states of the cells are subject to the rules of the transition function.

Transition Function

A global configuration of the automaton $S(n)$ (3) is a vector that contains the state values of all the cells in the set $V(G)$ at time n:

$$S(n) = \big(s(v_1,n), s(v_2,n), \ldots, s(v_{|V(G)|},n)\big)\,, \tag{8a}$$

$$S(n) = \big(s(v_i,n)_{v_i \in V(G)}\big)\,. \tag{8b}$$

The space containing all possible global configurations of the automaton is denoted by the letter $\mathscr{S}$ and is defined as $\mathscr{S} = \mathscr{E}^{|V(G)|}$. Then a global configuration takes one of the possible values of the space $\mathscr{S}$, o sea $S(n) \in \mathscr{S}$.

A local configuration of the automaton $S(v,n)$ (3) is a vector that contains the state values of an ordered subset of cells from the set $V(G)$ at time n.

$$S(v,n) = \big(s(v,n), s(w_1,n), \ldots, s(w_{|\mathscr{N}(v)|},n)\big)\,, \tag{9}$$

In this work, the ordered subset of cells is formed by a focal vertex v and its neighborhood $\mathscr{N}(v)$, that is:

$$S(v,n) = \big(s(v,n), s(w_i,n)_{w_i \in \mathscr{N}(v)}\big)\,. \tag{10}$$

However, it is necessary to be able to distinguish in a local configuration the vertices belonging to the immediate neighborhood (**??**) from those belonging to the distant neighborhood (**??**), as well as the vertices of each of the organs of the network. The implementation of the automaton must take these considerations into account.

The function $\mathscr{R}(S(v,n))$ (3) that receives a local configuration $S(v,n)$ centered on a focal vertex v at time n and returns the state of the vertex v at the next instant of time $n+1$ is called the local transition function.

$$\boxed{\mathscr{R} : \mathscr{E}^{|\mathscr{N}|} \to \mathscr{E}}\,, \tag{11a}$$

$$\boxed{\mathscr{R}(S(v,n)) = \begin{cases} e_1 & \text{con probabilidad } \rho(S(v,n) \to e_1) \\ e_2 & \text{con probabilidad } \rho(S(v,n) \to e_2) \\ \vdots & \cdots \\ e_{|\mathscr{E}|} & \text{con probabilidad } \rho(S(v,n) \to e_{|\mathscr{E}|}) \end{cases}}, \tag{11b}$$

where $e_i \in \mathscr{E},\ \forall i \in \{1,2,\ldots,|\mathscr{E}|\}$, $S(v,n) \in \mathscr{E}^{|\mathscr{N}|}$ y $\rho(S(v,n) \to e_i)$ is a transition probability that expresses the possibility of reaching the elementary state e_i from the local configuration $S(v,n)$. This transition probability satisfies the following conditions:

$$\rho : \mathscr{E}^{|\mathscr{N}|} \times \mathscr{E} \to [0,1], \tag{12a}$$

$$\sum_{i=1}^{|\mathscr{E}|} \rho(S(v,n) \to e_i) = 1. \tag{12b}$$

In a stochastic cellular automaton, the local transition function follows a probability distribution that determines the probability of changing the current state of a cell according to the configuration of its neighborhood. Thus, the state of a cell v at time $n+1$ is determined from its state at time n, by applying the corresponding local transition function.

$$s(v,n+1) = \mathscr{R}(S(v,n)). \tag{13}$$

The dynamics of the system are defined by a global transition function $\mathscr{R}_g(S(n))$ (3) that receives a global configuration of the automaton $S(n)$ at time n and is based on the application of the local transition function $\mathscr{R}(S(v,n))$ to all the cells of the automaton to obtain the global configuration at the next instant of time $n+1$.

$$\mathscr{R}_g : \mathscr{S} \to \mathscr{S}, \tag{14a}$$

$$\mathscr{R}_g(S(n)) = \mathscr{R}(S(v,n)) \quad \forall v \in V(G). \tag{14b}$$

Then the evolution of the automaton towards a global configuration at time $n+1$ is determined from the global configuration at time n, by applying the global transition function.

$$S(n+1) = \mathscr{R}_g(S(n)). \tag{15}$$

As shown in hypothesis VIII on tumor development in relation to the population, the model assumes that the dynamics of a tumor follow Verhulst's logistic growth function (6), presented below:

$$\begin{cases} \dfrac{dP}{dt} = rP(1 - \dfrac{P}{K}) \\ P(t=0) = P_0 \end{cases}, \tag{16}$$

where it is expressed that the variation of the population with respect to time depends on a growth rate r, the population P eat that instant of time and a value K that represents the carrying capacity, that is, the amount of individuals of the population that the environment can support. Angiogenesis can be translated as an increase in the loading capacity K of the environment, as well as an increase in the rate of cell proliferation due to the fact that neovascularization constitutes a more efficient supply method than nutrient diffusion. Therefore, the global growth dynamics will be described by two expressions: one corresponding to the avascular stage and one corresponding to the vascular stage, both with their particular parameters.

Tumor Growth Rules

One of the most important rules in defining the model is the rule that intervenes in the behavior of the cancerous cells that make up a tumorous mass.

The rule of the appearance of tumor cells, taking into account the new alternative transition probability, is written as:

$$s(v,n+1)=\mathscr{R}(S(v,n))=\begin{cases}\zeta_0(\tau(v,n,N_{tum})) & si\ s(v,n)=0\ \wedge\ \mathscr{N}_3^n(S(v,n))>0\\ \zeta_1(\tau(v,n,N_{tum})) & si\ s(v,n)=1\ \wedge\ \mathscr{N}_3^n(S(v,n))>0\\ \zeta_2(\tau(v,n,N_{tum})) & si\ s(v,n)=2\ \wedge\ \mathscr{N}_3^n(S(v,n))>0\end{cases}, \tag{17}$$

where the probability distribution of the random variables $\zeta_i(\tau(v,n,N_{tum}))\in\{i,3\}$ con $i\in\{0,1,2\}$ would remain as:

$$P(\zeta_i(\tau(v,n,N_{tum})=i)=1-\rho(\tau(v,n,N_{tum})\to 3), \tag{18a}$$

$$P(\zeta_i(\tau(v,n,N_{tum})=3)=\rho(\tau(v,n,N_{tum})\to 3). \tag{18b}$$

The calculation of the transition probability $\rho(\tau(v,n,N_{tum})\to 3)$ is defined from Verhulst's logistic growth equation. First, the growth equation should be written in such a way that we can express the variation of the population from an instant of time n to the instant $n+1$. For small values of Δt, the derivative of the growth equation can be approximated as:

$$\frac{dP(t)}{dt}\approx\frac{P(t+\Delta t)-P(t)}{\Delta t}, \tag{19a}$$

$$P'(t)\approx\frac{P(t+\Delta t)-P(t)}{\Delta t}, \tag{19b}$$

$$\Delta t P'(t)\approx P(t+\Delta t)-P(t), \tag{19c}$$

$$P(t+\Delta t)-P(t)\approx\Delta t P'(t), \tag{19d}$$

then if we take the time t as a discrete variable, and we make $t=n\Delta t$, we get:

$$P(n\Delta+\Delta t)-P(n\Delta t)\approx\Delta t P'(n\Delta t), \tag{20a}$$

$$P((n+1)\Delta t)-P(n\Delta t)\approx\Delta t P'(n\Delta t). \tag{20b}$$

The expression (20b) is interpreted as the variation of the tumor population population between the time instants n and $n+1$ as can be seen in the left part $P((n+1)\Delta t)-P(n\Delta t)$. The time that passes in the continuous model between the time instants n and $n+1$ of the cellular automaton is Δt. From (20b) it is inferred that the transition probability $\rho(\tau(v,n,N_{tum})\to 3)$ is calculated via $P'(t)$. Starting from (16), under the initial condition, it get (see appendix for the resolution process):

$$P(t)=\frac{P_0K}{P_0+(K-P_0)e^{-rt}}, \tag{21}$$

whose derivative $P'(t)$ finally takes the form (see appendix for the derivation process):

$$P'(t)=\frac{P_0Kre^{rt}(K-P_0)}{(P_0e^{rt}+K-P_0)^2}. \tag{22}$$

We previously exposed that the transition probability $\rho(\tau(v,n,N_{tum})\to 3)\in[0,1]$, which does not occur with the function $P'(t)$,so it is necessary to analyze its image. With this aim, we derive the function $P'(t)$ to seek the stationary points (see appendix for the derivation process), obtaining:

$$P''(t)=\frac{P_0Kr^2e^{rt}(P_0-K)(P_0e^{rt}+P_0-K)}{(P_0e^{rt}+K-P_0)^3}, \tag{23}$$

where it is inferred that $P'(t)$ possesses a maximum when:

$$t = \frac{1}{r} \ln \frac{K - P_0}{P_0}, \tag{24}$$

evaluating $P'(t)$ at this value of t we obtain the maximum growth probability:

$$P' \left(t = \frac{1}{r} \ln \frac{K - P_0}{P_0} \right) = \frac{Kr}{4}. \tag{25}$$

Therefore $P'(t)$ reaches its maximum value at the point $(\frac{1}{r} \ln \frac{K-P_0}{P_0}, \frac{Kr}{4})$, where this value depends directly on the loading capacity K and the growth rate r, returning the probability interval $[0, \frac{Kr}{4}]$.Suppose that ρ_{max} is the maximum value of the function $P'(t)$ in its domain, such that $P'(t) \in [0, \rho_{max}]$ subject to the condition $\rho_{max} \leq 1$. Solving the following inequality:

$$\frac{Kr}{4} \leq \rho_{max}, \tag{26}$$

we obtain the necessary condition for the function $P'(t) \in [0, \rho_{max}]$, resulting in:

$$r \leq \frac{4\rho_{max}}{K}. \tag{27}$$

By means of condition (27) it can be ensured that the tumoral growth probability obtained by evaluating $P'(t)$ belongs to the interval $[0, \rho_{max}]$,allowing an adjustment mechanism of the model through the appropriate selection of ρ_{max}. This adjustment mechanism is based on the fact that the models of cellular automata collected in previous works are divided into two general classes: those that reproduce a model specifically designed for the reproduction of tumor growth as (7), and those that reproduce a general growth model and adapt it to the specific case of tumor growth as (8; 9; 10), category to which this work belongs. In the second type of works it is common to find this mechanism in the form of a base probability as seen in (8). The condition 27 is expressed in terms of r since the value of ρ_{max} is selected a priori and K is determined directly from the available information about the growth process of a tumor, while the process of estimating r lacks a methodology so it is essential to have as much information as possible about its value.

From hypotheses VIII and XIV on tumor development in relation to the population and the interpretation of neovascularization respectively, it is inferred that the growth of the tumor population is described by two expressions corresponding to the avascular and vascular stages, each with its own growth rates r and loading capacities K. It can be deduced that both stages also have their own initial population values P_0, where the initial population of the vascular stage P_0^v corresponds to the loading capacity of the environment during the avascular stage K_a, that is, $K_a = P_0^v$. Similarly, a priori maximum probability values ρ_{max} can be defined for each of these stages. Finally, the transition probabilities, with $t = n\Delta t$, would remain as:

$$\rho_a(n\Delta t) = \frac{P_0^a K_a r_a e^{r_a n\Delta t}(K_a - P_0^a)}{(P_0^a e^{r_a n\Delta t} + K_a - P_0^a)^2}, \tag{28a}$$

$$\rho_v(n\Delta t) = \frac{P_0^v K_v r_v e^{r_v n\Delta t}(K_v - P_0^v)}{(P_0^v e^{r_v n\Delta t} + K_v - P_0^v)^2}. \tag{28b}$$

Thus, using the expressions (28a, 28b)and differentiating the stages of tumor development based on a new parameter n_a that indicates the duration of the avascular stage, we write the transition probability $\rho(\tau(v,n,N_{tum}) \to 3)$ as:

$$\rho(\tau(v,n,N_{tum}) \to 3) = \begin{cases} \rho_a(\tau(v,n,N_{tum})\Delta t) & si\ \tau(v,n,N_{tum}) \leq n_a \\ \rho_v((\tau(v,n,N_{tum}) - n_a)\Delta t) & si\ \tau(v,n,N_{tum}) > n_a \end{cases}. \tag{29}$$

Note in the expression for the calculation of ρ_v that the time used as a parameter is relative to the start of the vascular stage, that is, $\tau(v,n,N_{tum}) - n_a$. The expression (29) is known as the general transition probability of tumoral growth and is used as a basis for the definition of the specific probabilities for the displacement of each type of normal cell in the automaton.

Configuration and Parameters of the simulation.

Some of the parameters and configurations that can be modified are:

- S_x - Dimension of the space declared on the x-axis.
- S_y - Dimension of the space declared on the y-axis.
- S_z - Dimension of the space declared on the z-axis (1).

  The ranges of values for the spatial components of the graph vertices are as follows: $0 \leq x \leq S_x$, $0 \leq y \leq S_y$ y $0 \leq z \leq S_z$.
- p - Probability of reconnection in the Watts-Strogatz model
- P_0^a, P_0^v - Initial populations of the avascular and vascular stages respectively (1).
- Parameters corresponding to the number of states that the automaton cells can have and their descriptions.
- Parameters for possible transitions between the states of the automaton.
- Parameters for the probabilities of the transitions between states.

  When including parameters for the calculation of certain probabilities, one can take into account the calculation of the probability of interaction between tumor cells and the immune system (10).
- Parameters corresponding to the shape of the organs where the simulation will take place.
- Parameters to describe the schema of the organs where the simulation will be performed. This allows for the consideration of the characteristics of each organ separately and enables a more realistic simulation.

There are many other configurable parameters.

Results

The experiments and results obtained from these are essential for the validation of the computational model being developed. In this section, the obtained results are presented.

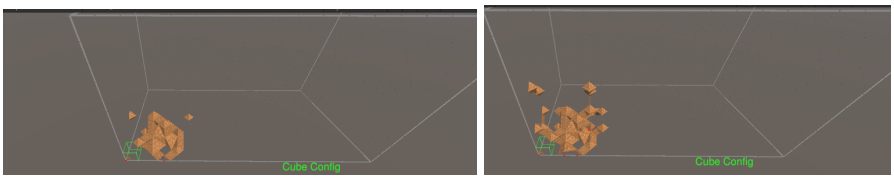

(a) Generation 4 (b) Generation 30

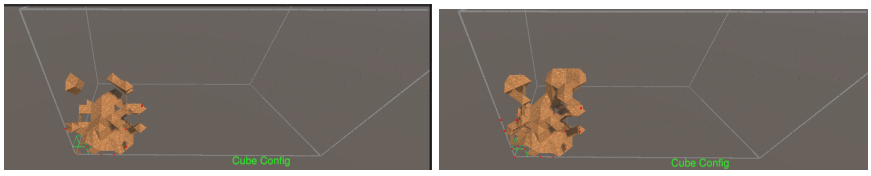

(c) Generation 45 (d) Generation 70

Figure 3: Visualizations of the cellular automaton simulation during the avascular stage. The area shown has dimension $[0,10.5]mm \times [0,10.5]mm \times [0,10.5]mm$.

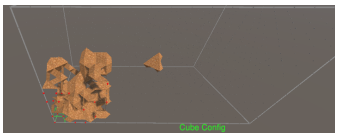

(a) Generation 150

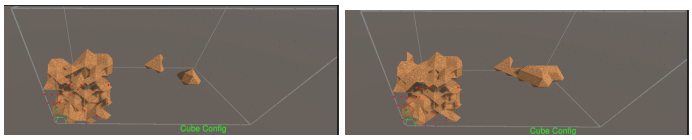

(b) Generation 175 (c) Generation 200

Figure 4: Visualizations of the cellular automaton simulation during the vascular stage. The tumor of larger area is the primary one and the one of smaller area is the secondary one that is carrying out the metastasis. The area shown has dimension $[0,52.5]mm \times [0,52.5]mm \times [0,52.5]mm$.

Conclusions

The growth of a tumor can be visualized in 3D using the Marching Cubes technique. It is widely used for medical visualizations, such as computed tomography (CT) and magnetic resonance imaging (MRI) images. Additionally, the Marching Cubes algorithm can reduce the computational time used for sampling in 3D reconstruction. However, one of the main issues with Marching Cubes is the presence of unused voxels that can be generated during the analysis of the coordinates and intensity values of 2D images. These unused voxels can affect the smoothness of the 3D surface (11).

The creation of a tool to simulate tumor growth using cellular automaton in any organ of the human body is a significant advancement in the field of modeling and simulation of biological systems. This tool provides an innovative and flexible approach to studying tumor growth, which has important implications in both basic research and clinical applications.

The ability to load specific configurations and adjust, add, or remove parameters that influence the realism of the simulation allows for the adaptation of the model to different scenarios and conditions. This makes the tool highly versatile and applicable to a wide range of situations and types of tumors.

The use of cellular automaton in tumor growth simulation allows for the accurate representation of the interaction between cells and their environment, as well as the temporal changes that occur. This modeling approach provides a detailed understanding of tumor growth dynamics and can be used to investigate various scenarios and conditions (3).

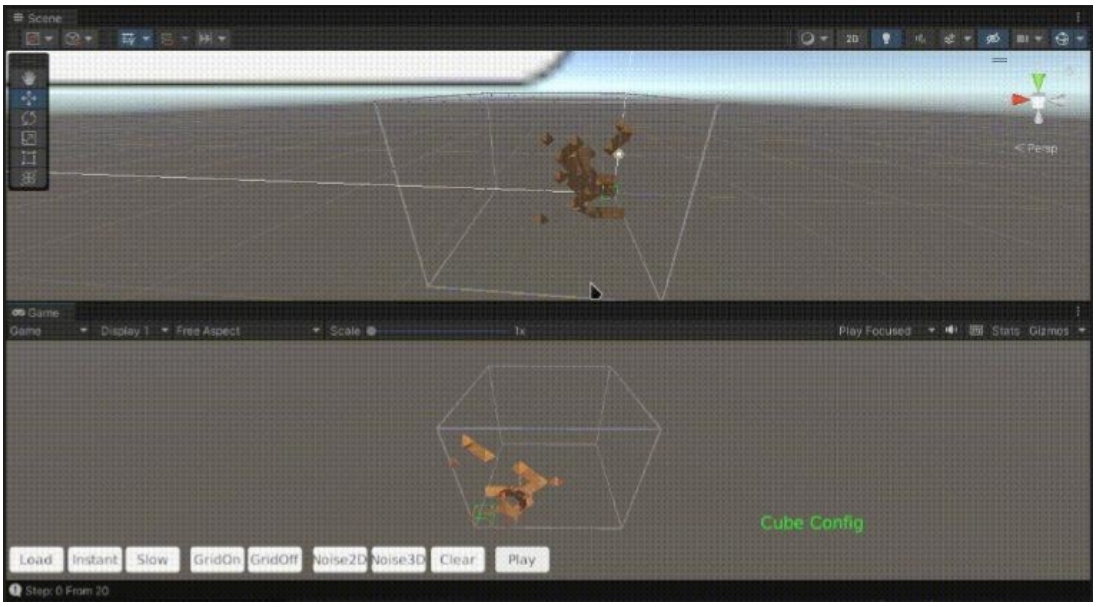

Figure 5: An example of simulating tumor growth in 3D at early stages.The code was developed in Unity

How much progress has been made so far?

- The loading and usage of parameters for the simulation have been implemented.
- The engine to simulate the growth of a tumor in small organs has been implemented.
- The cell graph with its connections has been visualized and analyzed.
- The size that the tumor will take during the simulation has been visualized.
- The code to render the shape the tumor will have has been implemented.5

What will be the focus in the next stages?

- Improving all of the above, for example, enhancing the implementation of 3D rendering using Marching Cubes to obtain smoother faces and triangles.
- Implementing changes between states following the details found in the literature.
- Implementing efficient algorithms to process large amounts of cells and their connections, we are talking about millions of both.
- Add Artificial Intelligence and Machine Learning techniques to obtain better approximations to reality.

Finally, the 3D visualization of tumor growth using the Marching Cubes technique can provide a valuable tool for healthcare professionals to better understand the dynamics of tumor growth and develop more effective treatment strategies.

Appendix

The following tools were used to develop this work: (5)

- For the generation of the simulation, C# in its .net7.0 version.
- For the visual part to visualize the cells and their connections in certain regions, Python in its 3.11 version with Streamlit and other dependencies.
- For the visual part to render the tumor, Unity in its 2021.3.28f1 version.

Figure 6: ”Example of an organ configuration file. It is indicated here which shape this region would have, indicating it in “shape”.

Figure 7: Example of a configuration file for the states that our cellular automaton would have.

Appendix A: Solution of the logistic growth equation subject to the initial conditions.

$$\begin{cases} \dfrac{dP}{dt} = rP(1-\dfrac{P}{K}) \\ P(t=0) = P_0 \end{cases}$$

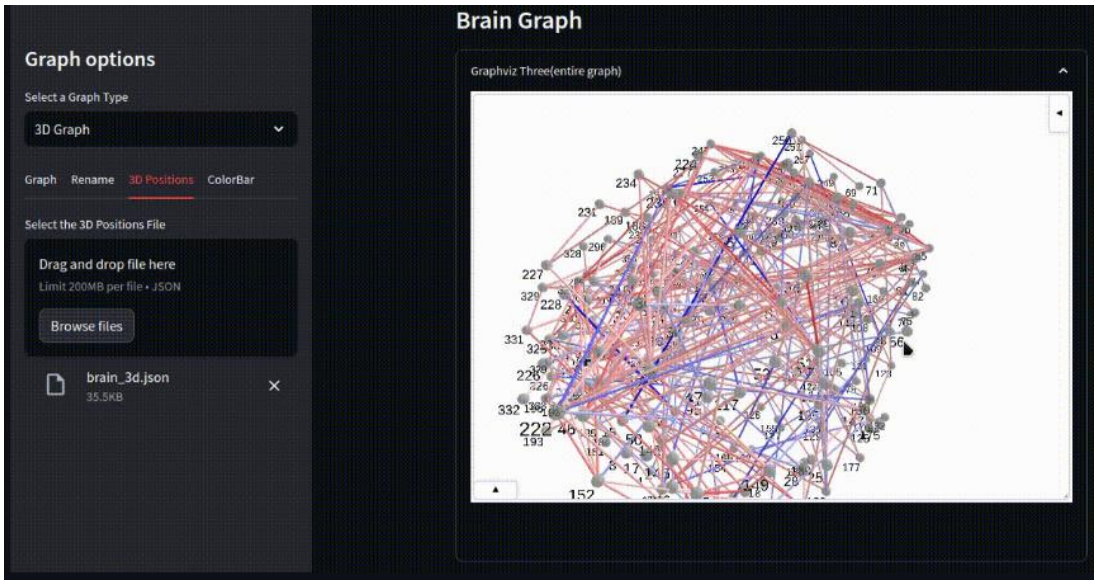

Figure 8: Visualization of cells and the connections between them.

(1.) $\frac{dP}{dt} = rP(1-\frac{P}{K})$

(2.) $rdt = \frac{dP}{P(1-\frac{P}{K})}$

(3.) $\int rdt = \int \frac{dP}{P(1-\frac{P}{K})}$

(4.) $\int rdt = \int \frac{1}{P}dP + \int \frac{\frac{1}{K}}{1-\frac{P}{K}}dP$
$*(u = 1-\frac{P}{K},\ du = -\frac{1}{K}dP)$

(5.) $rt + C = \ln P - \ln(1-\frac{P}{K})$

(6.) $e^{rt+C} = e^{lnP-\ln(1-\frac{P}{K})}$

(7.) $e^{rt+C} = \frac{e^{\ln P}}{e^{\ln(1-\frac{P}{K})}}$

(8.) $e^{rt}e^{C} = \frac{P}{1-\frac{P}{K}}$

(9.) $Ae^{rt} = \frac{P}{1-\frac{P}{K}}$

(10.) $P = \frac{AK}{Ke^{-rt}+A}$
$*(P(t=0) = P_0)$

(11.) $P_0 = \frac{AK}{K+A}$

(12.) $A = \frac{KP_0}{K-P_0}$

(13.) $P = \frac{\frac{KP_0}{K-P_0}K}{Ke^{-rt}+\frac{KP_0}{K-P_0}}$

$$\boxed{P(t) = \frac{P_0K}{P_0+(K-P_0)e^{-rt}}}$$

Appendix B: Derivation of the function P(t) for its use as a probability function.

$$\boxed{P(t) = \frac{P_0K}{P_0+(K-P_0)e^{-rt}}}$$

(1.) $P'(t) = \left[\frac{P_0K}{P_0+(K-P_0)e^{-rt}}\right]'$

(2.) $f = P_0K$

(3.) $f' = (P_0K)' = 0$

(4.) $g = P_0 + (K - P_0)e^{-rt} = P_0 + Ke^{-rt} - P_0e^{-rt}$

(5.) $g' = (P_0 + (K - P_0)e^{-rt})' = (P_0 + Ke^{-rt} - P_0e^{-rt})' = P_0re^{-rt} - Kre^{-rt}$

(6.) $g^2 = (P_0 + (K - P_0)e^{-rt})^2 = (P_0 + Ke^{-rt} - P_0e^{-rt})^2$

(7.) $P'(t) = \dfrac{P_0K(Kre^{-rt} - P_0re^{-rt})}{(P_0 + Ke^{-rt} - P_0e^{-rt})^2}$

(8.) $P'(t) = \dfrac{P_0K(re^{-rt}(K - P_0))}{(P_0 + Ke^{-rt} - P_0e^{-rt})^2}$

(9.) $P'(t) = \dfrac{P_0Kre^{-rt}(K - P_0)}{(P_0 + Ke^{-rt} - P_0e^{-rt})^2} \cdot \dfrac{e^{2rt}}{e^{2rt}}$

(10.) $P'(t) = \dfrac{P_0Kre^{rt}(K - P_0)}{(P_0e^{rt} - P_0 + K)^2}$

$$\boxed{P'(t) = \frac{P_0Kre^{rt}(K - P_0)}{(P_0e^{rt} - P_0 + K)^2}}$$

Appendix C: Derivation of the function P'(t) for the search of its stationary points.

$$\boxed{P'(t) = \frac{P_0Kre^{rt}(K - P_0)}{(P_0e^{rt} - P_0 + K)^2}}$$

(1.) $P''(t) = \left[\dfrac{P_0Kre^{rt}(K - P_0)}{(P_0e^{rt} - P_0 + K)^2}\right]'$

(2.) $f = P_0Kre^{rt}(K - P_0) = P_0K^2re^{rt} - P_0Kre^{rt}$

(3.) $f' = (P_0Kre^{rt}(K - P_0))' = P_0Kr^2e^{rt}(K - P_0) = P_0K^2r^2e^{rt} - P_0Kr^2e^{rt}$

(4.) $g = (P_0e^{rt} - P_0 + K)^2 = P_0^2e^{2rt} - 2P_0^2e^{rt} + 2P_0Ke^{rt} - 2P_0K + P_0^2 + K^2$

(5.) $g' = ((P_0e^{rt} - P_0 + K)^2)' = 2P_0^2re^{2rt} - 2P_0^2re^{rt} + 2P_0Kre^{rt}$

(6.) $g^2 = ((P_0e^{rt} - P_0 + K)^2)^2 = (P_0e^{rt} - P_0 + K)^4$

(7.) $P''(t) = \dfrac{3P_0^3K^2r^2e^{rt} + P_0K^4r^2e^{rt} + P_0^4Kr^2e^{3rt} - 3P_0^2K^3r^2e^{rt} - P_0^3K^2r^2e^{3rt} - P_0^4Kr^2e^{rt}}{(P_0e^{rt} - P_0 + K)^4}$

(8.) $P''(t) = \dfrac{P_0^3Kr^2e^{3rt}(P_0 - K) + 3P_0^2K^2r^2e^{rt}(P_0 - K) - P_0Kr^2e^{rt}(P_0^3 - K^3)}{(P_0e^{rt} - P_0 + K)^4}$

(9.) $P''(t) = \dfrac{(P_0 - K)(P_0^3Kr^2e^{3rt} + 2P_0^2K^2r^2e^{rt} - P_0K^3r^2e^{rt} - P_0^3Kr^2e^{rt})}{(P_0e^{rt} - P_0 + K)^4}$

(10.) $P''(t) = \dfrac{P_0Kr^2e^{rt}(P_0 - K)(P_0^2e^{2rt} + 2P_0K - K^2 - P_0^2)}{(P_0e^{rt} - P_0 + K)^4}$

(11.) $P''(t) = \dfrac{P_0Kr^2e^{rt}(P_0 - K)(P_0e^{rt} + P_0 - K)(P_0e^{rt} - P_0 + K)}{(P_0e^{rt} - P_0 + K)^4}$

(12.) $P''(t) = \dfrac{P_0 K r^2 e^{rt}(P_0 - K)(P_0 e^{rt} + P_0 - K)}{(P_0 e^{rt} - P_0 + K)^3}$

(13.) $0 = e^{rt}(P_0 - K)(P_0 e^{rt} + P_0 - K)$

(14.) $0 = P_0 e^{rt} + P_0 - K$

(15.) $e^{rt} = \dfrac{K - P_0}{P_0}$

(16.) $\ln e^{rt} = \ln \dfrac{K - P_0}{P_0}$

(17.) $rt = \ln \dfrac{K - P_0}{P_0}$

(18.) $t = \dfrac{1}{r} \ln \dfrac{K - P_0}{P_0}$

$$\boxed{P''(t) = \frac{P_0 K r^2 e^{rt}(P_0 - K)(P_0 e^{rt} + P_0 - K)}{(P_0 e^{rt} - P_0 + K)^3}} \qquad \boxed{t = \frac{1}{r} \ln \frac{K - P_0}{P_0}}$$

References

[1] D. Viera Barredo. Autómata celular estocástico en redes complejas para el estudio de la invasión, migración y metástasis del cáncer, June 2019.

[2] W. E. Lorensen and H. E. Cline. Marching cubes: A high resolution 3d surface construction algorithm. *ACM SIGGRAPH Computer Graphics*, 21(4):163–169, 1987.

[3] Andreas Deutsch, Philip K. Maini, and Sabine Dormann. *Cellular Automaton Modelling of Biological Pattern Formation: Characterization, Applications, and Analysis*. Birkhuser Boston, 2007.

[4] Duncan J. Watts and Steven H. Strogatz. Collective dynamics of small-world networks. *Nature*, 393:440–442, 1998.

[5] M. A. Cirne and H. Pedrini. Marching cubes technique for volumetric visualization accelerated with graphics processing units. *Journal of the Brazilian Computer Society*, 19:223–233, 2013.

[6] Pierre F. Verhulst. Notice sur la loi que la population poursuit dans son accroissement. *Correspondance mathématique et physique*, 10:113–121.

[7] Ruben Interian, Reinaldo Rodríguez-Ramos, Fernando Valdés Ravelo, Ariel Ramírez Torres, Celso C. Ribeiro, and Aura Conci. Tumor growth modelling by cellular automata. *Mathematics and Mechanics of Complex Systems*, 5(3-4):239–259, 2017.

[8] A. Kansal and Salvatore Torquato. Simulated brain tumor growth dynamics using a three-dimentional cellular automaton. *Journal of Theoretical Biology*, 203:367–382, 2000.

[9] Yang Jiao and Salvatore Torquato. Emergent behaviors from a cellular automaton model for invasive tumor growth in heterogeneous microenvironments. *Comput Biol*, 7(12), 2011. DOI:10.1371/journal.pcbi.1002314.

[10] Huricha Ruanxiaogang. A simple cellular automaton model for tumor-immunity system. In *Proceedings of the 2003 IEEE*, 2003.

[11] Porawat Visutsak. Marching cubes and histogram pyramids for 3d medical visualization. *Journal of Imaging*, 6, 2020. Available at: https://api.semanticscholar.org/CorpusID:225446991.